Memorias del Congreso Nacional de Control Automático
ISSN: 2594-2492

Nonlinear prediction-based smooth-bounded backstepping control for a quadrotor with input delay

M.A. Vallejo-Alarcón, M. Velasco-Villa, R. Castro-Linares

Department of Electrical Engineering, Mechatronics Section, CINVESTAV-IPN, Mexico City, Mexico, CP 07360. (e-mail: {mvallejoa, velasco, rcastro}@cinvestav.mx)

Abstract: In this paper, a trajectory-tracking prediction-based control strategy is presented for a quadrotor with input time-delays, using smooth-bounded error-correction actions. This is, a smooth-bounded backstepping-based control design is feed with prediction-based estimated states obtained using a full-state predictor; this scheme uses a quadrotor model reduced by an inner control loop also presented. The prediction-based control scheme is analyzed for stability and validated by numerical simulation results.

Keywords: UAVs, Quadrotor, Delay systems, Backstepping, Nonlinear control

1. INTRODUCTION

The quadrotor is a Unmanned Aerial Vehicle (UAV) that has gained research relevance due to its capabilities of Vertical Take-Off and Landing (VTOL) and omnidirectional flight (Tayebi and McGilvray, 2006; Mellinger and Kumar, 2011). This vehicle is subject of time-delays, either by remote communication, high processing latency, data dropout, or delayed state measurement, among others; the effects of this phenomena are mostly neglected in literature since the time-delay's extent tends to be relatively small; but, as this extent grows, the importance of compensating its effects rises, because it could cause incidental system damage.

To address control problems, as regulation, way-point tracking, or trajectory tracking, for the quadrotor, different approaches like PID, LQ, backstepping, sliding modes, or neural networks, have been boarded (Bouabdallah and Siegwart, 2005; Wang et al., 2018). Also, the problem of compensating time-delay effects in quadrotors has gained interest (Lozano et al., 2004; Sanz et al., 2017; Wang et al., 2018), as the analysis of delay-differential systems and the endeavors to attend them are a relevant subject in research (Niculescu, 2001; Kharitonov, 2013).

This paper presents a trajectory-tracking prediction-based backstepping control scheme with smooth-bounded error-correction actions for a quadrotor subject to input time-delays; this scheme comprises an embedded control loop for pitch and roll angles of a quadrotor, a state predictor, and a prediction-based controller. The embedded control loop, used to reduce the system's model, is taken as virtually delay-free, as it is considered to be executed on board using common quadrotor built-in capabilities.

The proposed state predictor requires bounded control signals in order to have stability, and it is used to feed the controller. A controller is designed under a backstepping approach, using bounded error-correction actions in order to fulfill the mentioned state predictor requirement. The stability of the resultant closed-loop system is analyzed. Also a numerical simulation is carried out to evaluate the performance of the control scheme.

The paper is organized as follows. Section 2 presents a quadrotor model and an embedded control loop. Section 3 presents the design of a state predictor together with a stability analysis. Section 4 presents the design and stability analysis of a prediction-based backstepping control with smooth-bounded error-correction actions. Section 5 presents a numerical evaluation of the proposed scheme, and Section 6 highlights some concluding remarks.

2. QUADROTOR DYNAMIC MODEL

The considered quadrotor model (García-Carrillo et al., 2013) uses the North-East-Down (NED) inertial frame to measure position and the so called Euler angles, roll, pitch, and yaw, to describe attitude; this is, respectively, the position is given by $\chi = [x, y, z]^T$ and the attitude by $\rho = [\phi, \theta, \psi]^T$, as it is shown in Fig. 1. The model is given by

$$\begin{aligned} \begin{bmatrix} \ddot{x}(t) \\ \ddot{y}(t) \end{bmatrix} &= -\left(f(t)/m\right) G(\psi(t)) \begin{bmatrix} \sin(\theta(t))\cos(\phi(t)) \\ \sin(\phi(t)) \end{bmatrix}, \\ \ddot{z}(t) &= g - \left(f(t)/m\right)\cos(\theta(t))\cos(\phi(t)), \\ H^T I H \ddot{\rho} &= H^T\left(IH\dot{\rho} \times H\dot{\rho}\right) - H^T I \dot{H}\dot{\rho} + H^T \nu, \end{aligned} \tag{1}$$

the cross product is represented as $\times$; also, m is the vehicle's mass, g is que gravitational acceleration constant, the inertia matrix is $I = \text{diag}\left\{I_{x_x}, I_{y_y}, I_{z_z}\right\}$.

The system's inputs are f and ν, with f the total rotor thrust, and $\nu = [\nu_\phi, \nu_\theta, \nu_\psi]^T$ the generalized torque. Moreover, with the matrices

$$G(\psi) = \begin{bmatrix} \cos(\psi) & \sin(\psi) \\ \sin(\psi) & -\cos(\psi) \end{bmatrix},$$
$$H = \begin{bmatrix} 1 & 0 & -\sin(\theta) \\ 0 & \cos(\phi) & \cos(\theta)\sin(\phi) \\ 0 & -\sin(\phi) & \cos(\theta)\cos(\phi) \end{bmatrix}.$$

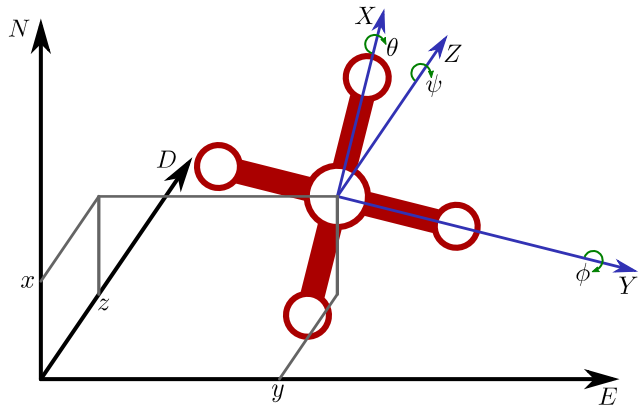

Fig. 1. Quadrotor in the NED inertial frame.

Model (1) uses the Euler angles representation, so it presents singularities; then, the next assumption is made.

Assumption 1. The pitch and roll angles are remaining bounded, such as $|\theta| < \pi/2$ and $|\phi| < \pi/2$.

Such an assumption does not restrict the operation of the quadrotor under usual parameters, since most of its common maneuvers are enclosed in such manner.

In order to reduce the notation, the right-side equation's time dependence is going to be obviated henceforth, with the exception of those dependencies with modifiers.

2.1 Embedded control loop

To keep the control scheme design close to the physical capabilities of these vehicles and reduce model (1), an inner control loop, to be executed on board, is designed using some common built-in capabilities. It is considered that the system has an Inertial Measurement Unit (IMU) measuring ϕ, θ, $\dot{\phi}$, $\dot{\theta}$, and $\dot{\psi}$.

Considering Assumption 1, initial inputs are chosen as

$$\begin{aligned} f(t) =& m(g - \tilde{\nu}_z)/(\cos(\theta)\cos(\phi)), \\ \nu(t) =& -IH\dot{\rho} \times H\dot{\rho} + I\dot{H}\dot{\rho} + IH\tilde{\nu}, \end{aligned} \tag{2}$$

with $\tilde{\nu}_z$ and $\tilde{\nu} = [\tilde{\nu}_\phi, \tilde{\nu}_\theta, \tilde{\nu}_\psi]^T$ new system inputs.

Then, the model is reduced to

$$\begin{bmatrix} \ddot{x}(t) \\ \ddot{y}(t) \end{bmatrix} = (\tilde{\nu}_z - g) G(\psi) \begin{bmatrix} \tan(\theta) \\ \tan(\phi)/\cos(\theta) \end{bmatrix},$$
$$\ddot{z}(t) = \tilde{\nu}_z, \ \ddot{\phi}(t) = \tilde{\nu}_\phi, \ \ddot{\theta}(t) = \tilde{\nu}_\theta, \ \ddot{\psi}(t) = \tilde{\nu}_\psi.$$

Desired roll and pitch angles, ϕ_d and θ_d, are considered to be received through wireless equipment. Assuming these signals as class C^2 functions, it is possible to define the tracking errors

$$e_\theta(t) = \theta_d - \theta, \qquad e_\phi(t) = \phi_d - \phi,$$

to set an embedded control loop as

$$\begin{aligned} \tilde{\nu}_\theta(t) =& \ddot{\theta}_d + k_{p_\theta} e_\theta + k_{d_\theta} \dot{e}_\theta, \\ \tilde{\nu}_\phi(t) =& \ddot{\phi}_d + k_{p_\phi} e_\phi + k_{d_\phi} \dot{e}_\phi, \end{aligned} \tag{3}$$

with $k_{p_\theta}, k_{d_\theta}, k_{p_\phi}, k_{d_\phi} > 0$ control gains. Then, the closed-loop dynamics for those errors are

$$\begin{aligned} \ddot{e}_\theta(t) =& -k_{p_\theta} e_\theta - k_{d_\theta} \dot{e}_\theta, \\ \ddot{e}_\phi(t) =& -k_{p_\phi} e_\phi - k_{d_\phi} \dot{e}_\phi; \end{aligned}$$

it is clear that this subsystem is exponentially stable using proper gains, so $\theta \to \theta_d$ and $\phi \to \phi_d$ exponentially; in such a manner that, for an outer control loop, one can consider that $\theta = \theta_d$, $\phi = \phi_d$.

Then, one can represent the system's model as

$$\begin{bmatrix} \ddot{x}(t) \\ \ddot{y}(t) \end{bmatrix} = (\tilde{\nu}_z - g) G(\psi) \begin{bmatrix} \tan(\theta_d) \\ \tan(\phi_d)/\cos(\theta_d) \end{bmatrix},$$
$$\ddot{z}(t) = \tilde{\nu}_z, \ \ddot{\psi}(t) = \tilde{\nu}_\psi;$$

so, to reduce this representation by canceling trigonometric functions, desired pitch and roll angles are defined as

$$\begin{aligned} \theta_d =& \arctan(\tilde{\nu}_x), \\ \phi_d =& \arctan\left(\tilde{\nu}_y \Big/ \sqrt{1 + \tilde{\nu}_x^2}\right), \end{aligned} \tag{4}$$

with $\tilde{\nu}_x$ and $\tilde{\nu}_y$ new system inputs. Thus, organizing the states in vector-states, as follows:

$$s_1 = \begin{bmatrix} z \\ \psi \end{bmatrix}, \ s_2 = \begin{bmatrix} \dot{z} \\ \dot{\psi} \end{bmatrix}, \ s_3 = \begin{bmatrix} x \\ y \end{bmatrix}, \ s_4 = \begin{bmatrix} \dot{x} \\ \dot{y} \end{bmatrix},$$

and arranging the inputs as $u_1 = [\tilde{\nu}_z, \tilde{\nu}_\psi]^T$, $u_2 = [\tilde{\nu}_x, \tilde{\nu}_y]^T$, one has the reduced model

$$\begin{aligned} \dot{s}_1(t) =& s_2, & \dot{s}_2(t) =& u_1, \\ \dot{s}_3(t) =& s_4, & \dot{s}_4(t) =& (\tilde{\nu}_z - g) G(\psi) u_2. \end{aligned} \tag{5}$$

2.2 Time-delayed input and time-advanced model

Now, consider a known time-delay $\tau > 0$ that appears in the inputs of (5), *i.e.* $u_1(t - \tau)$, $u_2(t - \tau)$, and let us define the time-advanced states

$$\begin{aligned} x_a(t) =& x(t + \tau), & y_a(t) =& y(t + \tau), \\ z_a(t) =& z(t + \tau), & \psi_a(t) =& \psi(t + \tau), \end{aligned}$$

also, associated with these, the state-vectors

$$a_1 = \begin{bmatrix} z_a \\ \psi_a \end{bmatrix}, \ a_2 = \begin{bmatrix} \dot{z}_a \\ \dot{\psi}_a \end{bmatrix}, \ a_3 = \begin{bmatrix} x_a \\ y_a \end{bmatrix}, \ a_4 = \begin{bmatrix} \dot{x}_a \\ \dot{y}_a \end{bmatrix},$$

one then has the time-advanced model

$$\begin{aligned} \dot{a}_1(t) =& a_2, & \dot{a}_2(t) =& u_1, \\ \dot{a}_3(t) =& a_4, & \dot{a}_4(t) =& (\tilde{\nu}_z - g) G(\psi_a) u_2. \end{aligned} \tag{6}$$

3. STATE PREDICTOR

Let us define the predicted states for x, $\dot{x}$, y, $\dot{y}$, z, $\dot{z}$, ψ, and $\dot{\psi}$ correspondingly as x_{p_1}, x_{p_2}, y_{p_1}, y_{p_2}, z_{p_1}, z_{p_2}, ψ_{p_1}, and ψ_{p_2}. Also, let us define the predicted state-vectors

$$a_{p_1} = \begin{bmatrix} z_{p_1} \\ \psi_{p_1} \end{bmatrix},\ a_{p_2} = \begin{bmatrix} z_{p_2} \\ \psi_{p_2} \end{bmatrix},\ a_{p_3} = \begin{bmatrix} x_{p_1} \\ y_{p_1} \end{bmatrix},\ a_{p_4} = \begin{bmatrix} x_{p_2} \\ y_{p_2} \end{bmatrix},$$

and, with these, the prediction errors

$$e_{p_j} = a_j - a_{p_j} = \left[e_{q_{(2j-1)}}, e_{q_{(2j)}}\right]^T,\ j = 1, \dots 4.$$

Then, one can construct a state predictor of the Luenberger type (1971),

$$\begin{aligned} \dot{a}_{p_1}(t) =& a_{p_2} + K_1 e_{p_1}(t-\tau), \\ \dot{a}_{p_2}(t) =& u_1 + K_2 e_{p_2}(t-\tau), \\ \dot{a}_{p_3}(t) =& a_{p_4} + K_3 e_{p_3}(t-\tau), \\ \dot{a}_{p_4}(t) =& (\tilde{\nu}_z - g) G(\psi_{p_1}) u_2 + K_4 e_{p_4}(t-\tau), \end{aligned} \tag{7}$$

with $K_j = \text{diag}\left\{k_{(2j-1)}, k_{(2j)}\right\} > 0$, $j = 1, \dots, 4$.

Besides, one may notice that

$$\alpha = G(\psi_a) - G(\psi_{p_1}) = 2\sin(e_{q_2}/2)\,\Upsilon,$$

with

$$\Upsilon = \begin{bmatrix} -\sin(\psi_{p_1} + e_{q_2}/2) & \cos(\psi_{p_1} + e_{q_2}/2) \\ \cos(\psi_{p_1} + e_{q_2}/2) & \sin(\psi_{p_1} + e_{q_2}/2) \end{bmatrix},$$

so, the prediction error dynamics are obtained as

$$\begin{aligned} \dot{e}_{p_1}(t) &= -K_1 e_{p_1}(t-\tau) + e_{p_2}, \\ \dot{e}_{p_2}(t) &= -K_2 e_{p_2}(t-\tau), \\ \dot{e}_{p_3}(t) &= -K_3 e_{p_3}(t-\tau) + e_{p_4}, \\ \dot{e}_{p_4}(t) &= -K_4 e_{p_4}(t-\tau) + \alpha q, \end{aligned} \tag{8}$$

where $q = (\tilde{\nu}_z - g) u_2$. These dynamics can be rewritten as

$$\dot{e}_{p_a}(t) = K_0 e_{p_a} + K_{a_1} e_{p_a}(t-\tau), \tag{9a}$$

$$\dot{e}_{p_b}(t) = K_0 e_{p_b} + K_{b_1} e_{p_b}(t-\tau) + \Delta, \tag{9b}$$

with the perturbation $\Delta = \left[0, 0, (\alpha q)^T\right]^T$, and

$$e_{p_a} = \left[e_{q_1}, e_{q_2}, e_{q_3}, e_{q_4}\right]^T, \quad K_{a_1} = \text{diag}\left\{-k_1, \dots, -k_4\right\},$$

$$e_{p_b} = \left[e_{q_5}, e_{q_6}, e_{q_7}, e_{q_8}\right]^T, \quad K_{b_1} = \text{diag}\left\{-k_5, \dots, -k_8\right\},$$

$$K_0 = \begin{bmatrix} 0 & 0 & 1 & 0 \\ 0 & 0 & 0 & 1 \\ 0 & 0 & 0 & 0 \\ 0 & 0 & 0 & 0 \end{bmatrix}.$$

The next assumption is now introduced to study the stability of system (9).

Assumption 2. The inputs u_1 and u_2 of (6) are bounded.

One can now give the following result on the stability of the predictor error dynamics (9).

Lemma 3. Consider the prediction error dynamics (9) associated with the state predictor (7) for the time-advanced quadrotor model (6). Then, under Assumptions 1 and 2, for positive constants k_i, the prediction errors exponentially converge to zero if and only if

$$\tau < \pi/2k_i\ ,\ i = 1, \dots, 8.$$

Proof. The subsystem (9a) is a retarded linear time-invariant system; then, it is exponentially stable if and only if its spectrum lies in the open left half-plane of the complex plane (Bellman and Cooke, 1963; Kharitonov, 2013). Its characteristic function is given by

$$\beta(\lambda) = \det\left(\lambda I_4 - K_0 - e^{-\lambda r} K_{a_1}\right) = \prod_{i=1}^{4} \left(\lambda + k_i e^{-\tau\lambda}\right),$$

with $I_n \in \mathbb{R}^{n\times n}$ an identity matrix. Then, using the Lambert $\mathcal{W}$ function (Corless et al., 1996), the spectrum of the subsystem (9a) is obtained as

$$\lambda_i = r^{-1}\mathcal{W}(-\tau k_i),\ i = 1, \dots, 4. \tag{10}$$

The Lambert $\mathcal{W}$ function is multivalued, but its rightmost branch is the only one of interest, which happens to be its principal branch (Shinozaki and Mori, 2006), noted as $\mathcal{W}_0$. Then, noticing that the arguments for $\mathcal{W}$ in (10) are strictly real, and according to the Lambert $\mathcal{W}$ function implementation (Corless et al., 1996), one has that

$$\text{Re}\left(\mathcal{W}_0(n)\right) < 0 \iff -\pi/2 < n < 0, n \in \mathbb{R}.$$

Thus, considering that $k_i > 0$ and $\tau > 0$, the spectrum of the subsystem (9a) lies in the open left half-plane of the complex plane if and only if $\tau k_i < \pi/2$.

For subsystem (9b), the unperturbed case ($\Delta = 0$), presents a form equivalent to (9a); so, it presents the same conditions for exponential stability.

Now, let us consider that $\Delta \neq 0$. Starting from the fact that $\|\Upsilon\| = 1$, since it is a rotation matrix, and knowing that $|2\sin(e_{q_2}/2)| \leq |e_{q_2}|$, one has that $\|\alpha\| \leq |e_{q_2}|$. From (9a) exponential stability (shown above), one also knows that $|e_{q_2}| \to 0$ exponentially.

On the other hand, q depends on the system's inputs ($\tilde{\nu}_z$, $\tilde{\nu}_x$, and $\tilde{\nu}_y$); so, under Assumption 2, $\|\alpha\| \to 0$ implies that $\|\alpha q(t)\| \to 0$. Consequently, Δ vanishes independently from the states in (9b), and the unperturbed subsystem's stability holds. ■

Remark 4. As the system's inputs depend on the states, and these are not bounded, Assumption 2 does not necessarily hold. So, further analysis is needed.

4. PREDICTION-BASED BACKSTEPPING CONTROL DESIGN

For (6), considering a_2 as the virtual input u_a, and a_4 as the virtual input u_b, one has

$$\begin{aligned} \dot{a}_1(t) &= u_a, & \dot{a}_2(t) &= u_1, \\ \dot{a}_3(t) &= u_b, & \dot{a}_4(t) &= (\tilde{\nu}_z - g) G(\psi_a) u_2. \end{aligned} \tag{11}$$

Then, defining the desired trajectory

$$s_{d_1}(t) = [z_d, \psi_d]^T, \qquad s_{d_3}(t) = [x_d, y_d]^T,$$

the tracking errors

$$e_1 = \left[e_{z_1}\ e_{\psi_1}\right]^T = s_{1_d} - s_1, \quad e_2 = \left[e_{z_2}\ e_{\psi_2}\right]^T = u_a - s_2,$$

$$e_3 = \left[e_{x_1}\ e_{y_1}\right]^T = s_{3_d} - s_3, \quad e_4 = \left[e_{x_2}\ e_{y_2}\right]^T = u_b - s_4,$$

and the future desired trajectory

$$a_{d_i}(t) = \left[p_{d_{(2i-1)}}, p_{d_{(2i)}}\right]^T = s_{d_i}(t+\tau), \quad i = 1, 3,$$

one can define the future tracking errors as

$$\begin{aligned} e_{f_1}(t) &= a_{d_1} - a_1, & e_{f_2}(t) &= u_a - a_2, \\ e_{f_3}(t) &= a_{d_3} - a_3, & e_{f_4}(t) &= u_b - a_4. \end{aligned} \tag{12}$$

From (11) and (12), the future tracking error dynamics are obtained as

$$\begin{aligned} \dot{e}_{f_1}(t) =& \dot{a}_{d_1} - u_a, \\ \dot{e}_{f_2}(t) =& \dot{u}_a - u_1, \\ \dot{e}_{f_3}(t) =& \dot{a}_{d_3} - u_b, \\ \dot{e}_{f_4}(t) =& \dot{u}_b - (\tilde{\nu}_z - g) G(\psi_a) u_2. \end{aligned} \tag{13}$$

Then, in order to establish a feedback with the predicted states, let us define the predicted errors

$$\begin{aligned} e_{s_1}(t) =& a_{d_1} - a_{p_1}, & e_{s_2}(t) =& u_a - a_{p_2}, \\ e_{s_3}(t) =& a_{d_3} - a_{p_3}, & e_{s_4}(t) =& u_b - a_{p_4}. \end{aligned} \tag{14}$$

The next assumption is made to define feedback for (13).

Assumption 5. The proposed control scheme is not imposing accelerations in the D axis equal or above gravity acceleration, such that $\tilde{\nu}_z < g$.

We then have the following result.

Lemma 6. Consider the future tracking error dynamics (13), associated with model (6) and the future tracking errors (12). Then, under Assumptions 1 and 5, moreover using the definition of the predicted tracking errors (14), for positive constants b_i, c_i, $i = 1, \ldots, 8$ and the feedback

$$\begin{aligned} u_a(t) =& \dot{a}_{d_1} + B_1 \tanh(C_1 e_{s_1}), \\ u_1(t) =& \dot{u}_a + B_2 \tanh(C_2 e_{s_2}), \\ u_b(t) =& \dot{a}_{d_3} + B_3 \tanh(C_3 e_{s_3}), \\ u_2(t) =& (\tilde{\nu}_z - g)^{-1} G(\psi_{p_1}) (\dot{u}_b + B_4 \tanh(C_4 e_{s_4})), \end{aligned} \tag{15}$$

with $B_j = \operatorname{diag}\left\{b_{(2j-1)}, b_{(2j)}\right\}$, $C_j = \operatorname{diag}\left\{c_{(2j-1)}, c_{(2j)}\right\}$, $j = 1, \ldots, 4$, the future tracking errors asymptotically converge to zero. Furthermore, for small enough errors, such that $\tanh\left(C_j e_{s_j}\right) \approx C_j e_{s_j}$, the convergence is also exponential.

Proof. Feedback (15) requires Assumption 5 to hold in order to avoid singularities. From (15) and (13), it is obtained

$$\begin{aligned} \dot{e}_{f_i}(t) =& -B_i \tanh(C_i e_{s_i}), \ i = 1, 2, 3, \\ \dot{e}_{f_4}(t) =& \dot{u}_b - G(\psi_a) G(\psi_{p_1}) (\dot{u}_b + B_4 \tanh(C_4 e_{s_4})). \end{aligned} \tag{16}$$

Then, it is proposed a Lyapunov candidate function for e_{f_1} and e_{f_2}, as

$$V_a(e_{f_1}, e_{f_2}) = \frac{1}{2} \sum\nolimits_{j=1}^{2} e_{f_j} B_j^{-1} e_{f_j};$$

so, one obtains its time derivative

$$\begin{aligned} \dot{V}_a(e_{f_1}, e_{f_2}) =& \sum\nolimits_{j=1}^{2} e_{f_j} B_j^{-1} \dot{e}_{f_j} \\ =& -\sum\nolimits_{j=1}^{2} e_{f_j} \tanh\left(C_j e_{s_j}(t)\right). \end{aligned}$$

From Lemma 3, one knows that $e_{p_i} \to 0$ $(i = 1, \ldots, 4)$ exponentially, then $a_{p_i} \to a_j$ alike; so, from definitions (14) and (12), one has that $e_{s_i} \to e_{f_i}$; thus, in this analysis

$$\dot{V}_a(e_{f_1}, e_{f_2}) = -\sum\nolimits_{j=1}^{2} e_{f_j} \tanh\left(C_j e_{f_j}(t)\right).$$

So, as the hyperbolic tangent function is a monotonically increasing odd function, together with $C_j > 0$, one can conclude that $\dot{V}_a < 0$; thus, the subsystems for e_{f_1} and e_{f_2} converge asymptotically to zero.

Now, small enough errors, such that

$$\tanh\left(C_j e_{f_j}\right) \approx C_j e_{f_j},$$

lead us to

$$\dot{e}_{f_j}(t) = -B_j C_j e_{f_j}, \ j = 1, 2,$$

then, the fact that $B_j C_j > 0$ makes the exponential convergence to zero evident.

Now, the subsystems for e_{f_3} and e_{f_4} are considered. From Lemma 3, it is known that $\psi_{p_1} \to \psi_a$ exponentially; so, $G(\psi_a) G(\psi_{p_1}) \to I_2$ alike. Then, with analysis purposes, the subsystem can be written as

$$\begin{aligned} \dot{e}_{f_3}(t) =& -B_3 \tanh(C_3 e_{s_3}), \\ \dot{e}_{f_4}(t) =& -B_4 \tanh(C_4 e_{s_4}); \end{aligned}$$

thus, these subsystems meet the stability conditions presented before. ■

Remark 7. It must be noticed that the asymptotic convergence presented in Lemma 6 enables exponential convergence as the errors approach zero. This is, as the hyperbolic tangent function argument becomes smaller the function result becomes closer to the argument itself; this approximation turns out to be at least 99% accurate with argument values between -0.1742 and 0.1742.

Now, in order to analyze Assumption 2 claims, it is necessary to characterize the control signals u_1 and u_2 in (15). It must be noticed that the future desired trajectories a_{d_1} and a_{d_3} can be defined properly to met some given requisites; then, the next assumption holds.

Assumption 8. The desired trajectories are bounded as $\|\dot{a}_{d_1}\| < m_1$, $\|\ddot{a}_{d_1}\| < m_2$, $\|\dot{a}_{d_3}\| < m_3$, and $\|\ddot{a}_{d_3}\| < m_4$, for some positive constants m_i, $i = 1, \ldots, 4$.

Then, let us analyze the virtual input signals u_a and u_b. We know that $|\tanh(m)| < 1$, so

$$\left\|B_j \tanh\left(C_j e_{s_j}(t)\right)\right\| < \|B_j\|, j = 1, 3;$$

then, as Assumption 8 holds, $\left|\dot{a}_{d_j}\right| < m_j$, so

$$\begin{aligned} |u_a| &< m_1 + \|B_1\|, \\ |u_b| &< m_3 + \|B_3\|. \end{aligned}$$

Finally, let us analyze the input signals u_1 and u_2. Expanding terms of u_1, one has

$$\begin{aligned} u_1(t) =& \dot{u}_a + B_2 \tanh(C_2 e_{s_2}) \\ =& \ddot{a}_{d_1} + B_1 C_1 \left(I_2 - \tanh^2(C_1 e_{s_1})\right) \cdot \\ & \cdot (\dot{a}_{d_1} - a_{p_2} + K_1 e_{p_1}(t - \tau)) + B_2 \tanh(C_2 e_{s_2}). \end{aligned}$$

It is clear that

$$\|B_1C_1\left(I_2-\tanh\left(C_1e_{s_1}\right)\right)\|<2\,\|B_1\|\,\|C_1\|\,;$$

then, from Lemma 3, it is known that $e_{p_1}\to 0$ and $a_{p_2}\to a_2$, and from Lemma 6 one can conclude that $e_{s_2}\to 0$ and $a_2\to\dot{a}_{d_1}$, so $a_{p_2}\to\dot{a}_{d_1}$; then, $u_1\to\ddot{a}_{d_1}$ and as $\|\ddot{a}_{d_1}\|<m_2$, one has that the control signal u_1 converges to boundedness.

Then, analogously to u_1, one expands terms for u_2 as

$$u_2\left(t\right)\to\left(\tilde{\nu}_z-g\right)^{-1}G\left(\psi_{p_1}\right)\ddot{a}_{d_3};$$

also, Assumption 5 leads to the bound $\left|\left(\tilde{\nu}_z-g\right)^{-1}\right|<m_5$, for some positive constant m_5. Since $\|G\left(\psi_{p_1}\right)\|=1$, one has that $\left\|\left(\tilde{\nu}_z-g\right)^{-1}G\left(\psi_{p_1}\right)\right\|<m_5$; so, the control signal u_2 also converges to boundedness.

Remark 9. The proposed control law (15) establishes error-correction bounds by means of b_i, $i=1\ldots,8$, control gains, and sets the error-correction-action growrate by means of c_i.

Remark 10. The proposed control law (15) does not directly limit the control actions due to a desired trajectory, but it needs that the desired trajectory present bounds to make Assumptions 5 and 8 hold; as these bounds are free, they must be chosen such that they not overpass the capabilities of the used quadrotor.

5. CONTROL SCHEME NUMERICAL EVALUATION

Numerical evaluation was carried out in order to test the performance of the proposed control scheme. The numerical simulations were implemented in the *Simulink*® package of *MathWorks*® *Matlab*® with a fourth order Runge-Kutta numerical integrator, with a fixed integration step of 1ms.

5.1 Numerical scheme setup

The numerical simulation scheme comprises four segments. The first one is the quadrotor model (1), that is implemented by a Runge-Kutta 4 numerical integrator. The second one is the embedded attitude control represented by (2), (3), and (4), as it is presented in Section 2. The third one is the control law (15), whose output signals are time-delayed in order to be given to the second segment. The last segment is the state predictor (7), used to feed the control law in the third segment. This simulation scheme is depicted in Fig. 2.

The elected time-delay is $\tau=0.1$s. The prediction gains were chosen as $k_i=e^{-1}/\tau$, $i=1,\ldots,8$, in order to generate the leftmost eigenvalues (Corless et al., 1996), and the control gains were elected as $b_i=2$, $c_i=5$.

5.2 Numerical simulation results

The desired trajectory was designed as

$$\begin{aligned} x_d&=\sin\left(t\pi/5\right)/2, & y_d&=\sin\left(2t\pi/5\right)/2,\\ z_d&=-1-\sin\left(t\pi/10\right)/2, & \psi_d&=\sin\left(t\pi/20\right)/2, \end{aligned}\quad(17)$$

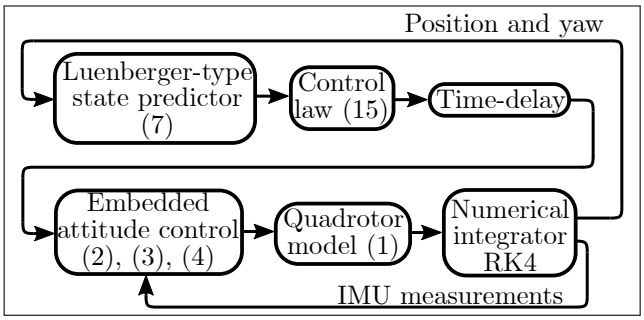

Fig. 2. Numerical simulation scheme.

this trajectory smoothly starts at $t=5$s and ends at $t=45$s, taking off and landing before and after these events, as it is depicted in Fig. 4

The desired trajectory (17) is a Three-dimensional (3D) lemniscate-like trajectory with yaw angle additional panning, describing a lemniscate type trajectory in the NE and ND planes; this is depicted in Fig. 3 where NE, ND, ED plane projections are presented along with a NED trajectory trace.

Using the control scheme as described above, and the desired trajectory (17), Figures 3, 4, and 5 were obtained. Figure 3 presents three trajectory traces in the NED inertial frame, that are the desired, predicted, and simulated trajectories; also shows the trajectory traces projected over NE, ND, and ED planes, in order to depict clearly the 3D trajectories.

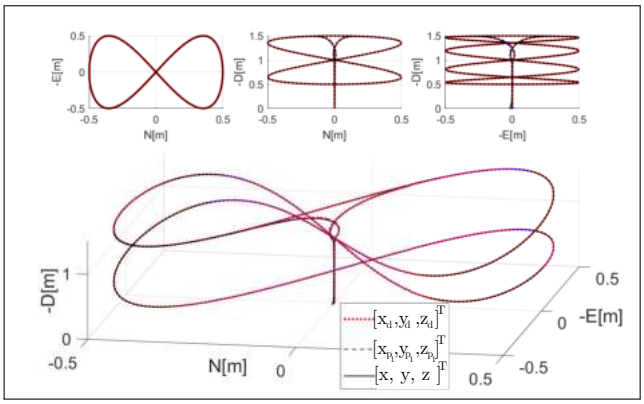

Fig. 3. Desired, predicted and simulated 3D trajectory traces, and plane projections.

Figure 4 shows the desired, predicted, and simulated trajectories of the position and yaw, plotted versus time. Finally, Fig. 5 presents in a synthetic manner the tracking and prediction errors, showing the vectorial norms of the tracking and prediction errors for the position, and the tracking and prediction yaw errors; with

$$e_{\xi_1}=\left\|\left[e_{x_1},e_{y_1},e_{z_1}\right]^T\right\|,\qquad e_{q_\xi}=\left\|\left[e_{q_5},e_{q_6},e_{q_1}\right]^T\right\|.$$

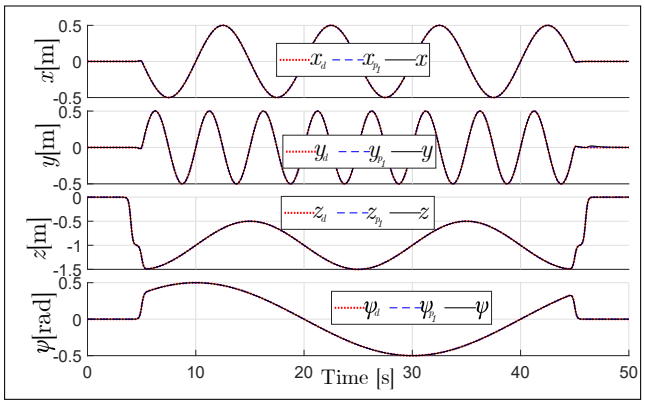

Fig. 4. Desired, predicted, and simulated, trajectory time-plots for position and yaw.

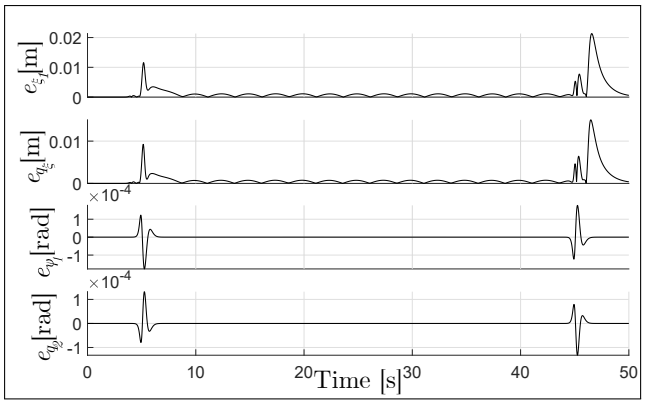

Fig. 5. Synthetic tracking and prediction errors for position and yaw.

Numerical evaluation results discussion. In Figures 3 and 4 can be observed the trajectories traced by the simulation scheme; but, as the control scheme maintains the tracking and prediction errors close to zero, it is hard to notice differences between desired, predicted, and simulated, trajectory plots. Then, Fig. 5 shows the tracking and prediction errors; these errors grow with the trajectory start and end ($t = 5$s and $t = 45$s), maintaining values close to zero otherwise.

6. CONCLUSION

In this paper was presented a prediction-based control scheme, designed with a backstepping approach using smooth-bounded error-correction actions, for a quadrotor with an embedded control loop and communication time-delays. Stability results were presented for a state predictor and a backstepping-based control design, presenting conditions for convergence and some needed assumptions. A numerical evaluation scheme was depicted and simulation results were presented, showing an adequate performance and error convergence for 3D trajectory tracking for a quadrotor with input time-delays.

ACKNOWLEDGEMENTS

This work was partially supported by the National Council for Science and Technology, CONACyT - Mexico, under the grant 254329.

REFERENCES

Bellman, R. and Cooke, K.L. (1963). Differential-difference equations. Technical Report R-374-PR, Rand Corporation, Santa Monica, CA.

Bouabdallah, S. and Siegwart, R. (2005). Backstepping and sliding-mode techniques applied to an indoor micro quadrotor. In *Proceedings of the 2005 IEEE international conference on robotics and automation*, 2247–2252. IEEE. doi:10.1109/ROBOT.2005.1570447.

Corless, R.M., Gonnet, G.H., Hare, D.E., Jeffrey, D.J., and Knuth, D.E. (1996). On the lambert w function. *Advances in Computational mathematics*, 5(1), 329–359. doi:10.1007/BF02124750.

García-Carrillo, L.R., Dzul-López, A.E., Lozano, R., and Pégard, C. (2013). *Quad Rotorcraft Control: Vision-Based Hovering and Navigation*, chapter 2, 32–34. Springer. doi:10.1007/978-1-4471-4399-4.

Kharitonov, V.L. (2013). *Time-delay systems: Lyapunov functionals and matrices*. Control Engineering. Birkhäuser, Boston. doi:10.1007/978-0-8176-8367-2.

Lozano, R., Castillo, P., Garcia, P., and Dzul, A. (2004). Robust prediction-based control for unstable delay systems: Application to the yaw control of a mini-helicopter. *Automatica*, 40(4), 603–612. doi:10.1016/j.automatica.2003.10.007.

Luenberger, D. (1971). An introduction to observers. *IEEE Transactions on Automatic Control*, 16(6), 596–602. doi:10.1109/TAC.1971.1099826.

Mellinger, D. and Kumar, V. (2011). Minimum snap trajectory generation and control for quadrotors. In *Robotics and Automation (ICRA), 2011 IEEE International Conference on*, 2520–2525. IEEE. doi:10.1109/ICRA.2011.5980409.

Niculescu, S.I. (2001). *Delay effects on stability: a robust control approach*. Springer-Verlag, London. doi:10.1007/1-84628-553-4.

Sanz, R., Garcia, P., Zhong, Q.C., and Albertos, P. (2017). Predictor-based control of a class of time-delay systems and its application to quadrotors. *IEEE Transactions on Industrial Electronics*, 64(1), 459–469. doi:10.1109/TIE.2016.2609378.

Shinozaki, H. and Mori, T. (2006). Robust stability analysis of linear time-delay systems by lambert w function: Some extreme point results. *Automatica*, 42(10), 1791–1799. doi:10.1016/j.automatica.2006.05.008.

Tayebi, A. and McGilvray, S. (2006). Attitude stabilization of a vtol quadrotor aircraft. *Control Systems Technology, IEEE Transactions on*, 14(3), 562 – 571. doi:10.1109/TCST.2006.872519.

Wang, X., Sun, C., Lin, X., and Yu, Y. (2018). Adaptive neural network control of a quadrotor with input delay. In *2018 Chinese Automation Congress (CAC)*, 4095–4100. IEEE. doi:10.1109/CAC.2018.8623376.